EUROPEAN JOURNAL OF ENTOMOLOGY
ISSN (online): 1802-8829
http://www.eje.cz
Eur. J. Entomol. **119**: 23–35, 2022
doi: 10.14411/eje.2022.003
ORIGINAL ARTICLE

RNA interference-based characterization of *Caspar*, *DREDD* and *FADD* genes in immune signaling pathways of the red flour beetle, *Tribolium castaneum* (Coleoptera: Tenebrionidae)

KAKERU YOKOI[1, 2, *], WATARU ITO[1, *], DAIKI KATO[1] and KEN MIURA[1]

[1] Applied Entomology Laboratory, Graduate School of Bioagricultural Sciences, Nagoya University, Furo-cho, Chikusa, Nagoya 464-8601, Japan; e-mails: yokoi123@affrc.go.jp, wataru-ito@agr.nagoya-u.ac.jp, daiki-kato@agr.nagoya-u.ac.jp, k-miura@agr.nagoya-u.ac.jp

[2] Insect Design Technology Group, Division of Insect Advanced Technology, Institute of Agrobiological Sciences, NARO, Owashi, Tsukuba 305-8643, Japan

Key words. Anti-microbial peptide, IMD pathway, Toll pathway

Abstract. We previously demonstrated that two immune signaling pathways, Toll and IMD, were concomitantly activated in the model beetle *Tribolium castaneum* by challenges to their immune system by several species of microbes, including Gram-positive and -negative bacteria as well as yeast. This contrasts with the *Drosophila* immune system in which more specific pathway activation depending on the type of microbe is well established. We suggest that the activation of an indiscriminate immune pathway in *T. castaneum* is due in part to an unselective recognition of pathogen-associated molecular patterns by the extracellular sensing modules of the two pathways. In order to obtain a more detailed understanding of the *T. castaneum* immune pathway, we investigated whether potential components of the *T. castaneum* IMD pathway, *Caspar*, *DREDD* and *FADD*, are involved in immune reactions triggered by microbial challenges. A sequence analysis of these three genes with the orthologues of other species, including insects, mouse and human, indicated that *T. castaneum Caspar*, *DREDD* and *FADD* functioned as immune signal transducers, which are usually induced by microbial challenges. However, these genes were not induced by microbial challenges. To establish whether these genes are involved in immune reactions, we used RNA interference-mediated knockdown of these genes to assess the microbial induction levels of the representative read-out antimicrobial peptide genes of the respective classes. The results indicated that these genes encode the canonical constituents of the IMD pathway of this beetle. *DREDD* and *FADD* influenced the induction of Toll-dependent antimicrobial peptide genes, providing novel crosstalk points between the two immune pathways, which appears to support indiscriminate pathway activation in *T. castaneum*. Furthermore, the phenotypes of *DREDD* or *FADD* knockdown pupae challenged by the two model bacterial pathogens correlated with AMP gene induction in the respective knockdowns, indicating that these intracellular factors contributed to antibacterial host defenses.

INTRODUCTION

The insect immune system is solely composed of innate immune reactions that utilize germ line-encoded receptors to detect the invasion of several distinct pathogens (Hultmark, 2003; Ferrandon et al., 2007; Lemaitre & Hoffmann, 2007). When recognized, invading pathogens are attacked by a battery of innate immune responses. Insect immune responses as well as vertebrate immune responses may be conveniently divided into cellular and humoral immunities, the latter of which involves the systemic and robust production of antimicrobial peptides (AMPs) as a major and well-characterized response. Intensive studies on the model organism *Drosophila melanogaster* (Meigen) over the past two decades have delineated the paths and factors that uphold the AMP production response as one of the hallmarks of insect immunity.

Extracellular pathogen recognition leads to the activation of two signaling pathways in *Drosophila*, the Toll and IMD pathways (Valanne et al., 2011; Kleino & Silverman, 2014). The Toll pathway is mainly activated by either Lys-type peptidoglycan associated with most Gram-positive bacteria or fungal β-1,3 glucan, and the recognition of these two pathogen-associated molecular patterns (PAMPs) in circulation is mainly executed by peptidoglycan recognition protein SA (PGRP-SA) and Gram-negative binding protein 3, respectively (Gobert et al., 2003; Gottar et al., 2006). PAMP binding to these receptors subsequently activates a downstream serine protease cascade, which leads to the proteolytic activation of the Toll ligand Spät-

* These authors equally contributed.

zle (Spz) (Weber et al., 2003). Two Toll receptors, bound by two processed Spz dimers, undergo a conformational change and recruit the adaptor protein MyD88 through intracellular TID domains (Gangloff et al., 2008). This interaction also recruits another adaptor protein, Tube and the kinase Pelle via death domain (DD)-mediated interactions to form a heterotrimer complex comprising MyD88, Tube and Pelle (Sun et al., 2002). The formation of heterotrimers leads to the phosphorylation and degradation of Cactus, a *Drosophila* inhibitor of NF-κB, through paths that are not yet identified, and the NF-κB class transcription factor Dif or Dorsal translocates into the nucleus and activates a set of targets, including several AMP genes (Wu & Anderson, 1998).

Gram-negative bacterial infections preferentially activate the IMD pathway (Kleino & Silverman, 2014). *Meso*-diaminopimelic acid (DAP)-type peptidoglycan associated with Gram-negative bacteria and Gram-positive bacilli are mainly sensed by the membrane-bound receptor, PGRP-LC (Choe et al., 2002, 2005). Ligand binding may promote the dimerization or multimerization of PGRP-LC, and its cytoplasmic portion, harbouring the receptor-interacting protein homeotypic interaction motif, interacts with the adaptor protein IMD (Kaneko et al., 2006). IMD recruits the initiator caspase-8 homolog DREDD via the adaptor function of FADD (Leulier et al., 2000; Naitza et al., 2002), and DREDD is activated by mechanisms that have yet to be completely defined, but include K63 polyubiquitination by the E3 ubiquitin ligase DIAP2 (Meinander et al., 2012). Activated DREDD cleaves IMD at Asp^{30}, which exposes the interaction interface to DIAP2, and cleaved IMD is also subjected to K63 ubiquitination (Paquette et al., 2010). The polyubiquitin chain recruits and activates the kinase TAK1, which, in turn, activates the JNK and IKK branches of the IMD pathway (Rutschmann et al., 2000; Silverman et al., 2000, 2003). The *Drosophila* IKK complex comprises catalytic IKKβ and regulatory IKKγ subunits. The IKK complex is thought to phosphorylate another NF-κB class transcription factor, Relish (Stöven et al., 2000; Stöven et al., 2003). Phosphorylated Relish is then translocated into the nucleus after the proteolytic removal of its ankyrin portion by DREDD, ultimately activating its target genes.

While *Drosophila* immune signaling events leading to the activation of humoral responses have been examined in detail, comprehensive information on other insect species, particularly non-dipteran insects, is limited. This may be attributed to the unavailability of genomic information, except for some model insects, and also to the incompatibility of genetic manipulation techniques, including RNA interference (RNAi) in some experimental systems. Therefore, some of the information obtained on immune responses in non-*Drosophila* insects may be annotated on the basis of the *Drosophila* framework.

We started research on insect immune signaling using the model beetle *Tribolium castaneum* (Herbst) because information on its genome is available and this beetle exhibits systemic RNAi responses, and our aim was to provide another framework for an insect immune system (Tomoyasu et al., 2008; Tribolium Genome Sequencing Consortium, 2008). In the initial phase, we characterized all nine AMP genes in the genome of *T. castaneum* and categorized them into IMD pathway-dependent group I, Toll pathway-dependent group III, and co-dependent group II as well as non-inducible group IV genes by utilizing the RNAi of the pathway-specific intracellular adaptor protein genes, *IMD* and *MyD88* (Yokoi et al., 2012b). We subsequently demonstrated that epistatic relationships between the pathways and subclasses of NF-κB transcription factors in *Drosophila* were also present in *T. castaneum* (Yokoi et al., 2012a). Collectively, these findings indicated that the Toll and IMD pathways exist in this beetle, and we also noted that the specificity of pathway activation was distinct from that in *Drosophila* because the target AMP genes of both pathways were concomitantly activated by any of the five microbial species used, including Gram-negative and -positive bacteria as well as budding yeast. We considered this indiscriminate pathway activation to be a distinct feature of *T. castaneum* immune signaling, which differs from that of *Drosophila*, and we have been investigating the molecular mechanisms that support this phenomenon. We demonstrated that *PGRP-LA* encodes the canonical receptor of the IMD pathway in this beetle, and also that this isoform recognizes both Gram-positive and -negative bacteria (Koyama et al., 2015). The finding of extracellular pathogen recognition may account in part for the aforementioned immune pathway activation with lower specificity. In the present study, to extend our understanding of the *T. castaneum* immune system, we focused on potential receptor-proximal intracellular components in the IMD pathways of *T. castaneum*, *DREDD* and *FADD*, as well as the *DREDD* inhibitor *Caspar* (Kim et al., 2006), and investigated whether these factors provide bifurcating points of immune signaling and are involved in immune reactions against bacterial infections.

MATERIALS AND METHODS

Insect rearing

T. castaneum was reared on whole wheat flour at 30°C in the dark and their pupae were prepared as previously described (Yokoi et al., 2012b).

Microbes and injections into insects

Escherichia coli DH5α, *Micrococcus luteus* ATCC4698 and the budding yeast, *Saccharomyces cerevisiae* S288C were used as heat-killed cell suspensions with defined O.D. values, as described in Yokoi et al. (2012a). Prepared suspensions of *E. coli*, *M. luteus* and *S. cerevisiae* were 2.9×10^8, 2.9×10^7 and 5×10^6 cells/ml, respectively. Fifty nanolitres of heat-killed suspensions was injected into naïve or double strand RNA (dsRNA)-treated day 3 pupae using Nanoject II (Drummond Scientific Company) to elicit immune responses. Suspensions of live *Enterobacter cloacae* and *Bacillus subtilis* were also prepared and used in survival assays, as previously described in Yokoi et al. (2012b). *E. cloacae* and *B. subtilis* were generous gifts from Dr. Y. Yagi of Nagoya University. *S. cerevisiae* S288C was from Dr. T. Ushimaru of Shizuoka University. *M. luteus* ATCC4698 was provided by the RIKEN Bioresource Center in Japan.

Genes examined in the present study

The following *T. castaneum* gene sequences from reference genome version Tcas2.0 were retrieved from Tcas2.0/annotation/TCGleanPrediction data (URL: ftp://ftp.hgsc.bcm.edu/Tcastaneum/) available at "BCM-HGSC data" in the "Red Flour Beetle Genome Project" site (URL: https://www.hgsc.bcm.edu/arthropods/red-flour-beetle-genome-project) and utilized in the present study (Zou et al., 2007; Tribolium Genome Sequencing Consortium, 2008): *Caspar* (Gene ID in gene set data: GLEAN_09985); *DREDD* (GLEAN_14026); *FADD* (GLEAN_14042); *Attacin 1* (*Att1*) (GLEAN_07737); (GLEAN_07739); *Cecropin 2* (*Cec2*) (GLEAN_00499); *Cecropin 3* (*Cec3*) (GLEAN_00500); *Coleoptericin 1* (*Col1*) (GLEAN_05093 and GLEAN_10517: *Col1* was split into two genes in gene set data.); *Defensin 3* (*Def3*) (GLEAN_12469); *IMD* (GLEAN_10851); and the normalizer gene for qRT-PCR analyses, *ribosomal protein L32* (*RPL32*) (GLEAN_06106).

Real-time quantitative RT-PCR (qRT-PCR)

Total RNA was extracted from the whole body of *T. castaneum* pupae using TRIZOL reagent (Invitrogen). After spectrophotometric scanning and assessments, 0.5 µg of total RNA was converted to first-strand cDNA utilizing a PrimeScript RT Reagent Kit with gDNA Eraser (TAKARA), and first-strand cDNA was analysed by qRT-PCR using the SYBR Premix Ex Taq Perfect Real Time Kit Tli RNAaseH Plus (TAKARA) and Thermal Cycler Dice Real Time System (Model TP800, TAKARA). The sequences of primer pairs used for qRT-PCR of *Caspar*, *DREDD* and *FADD* are shown in the Supplementary Table 1. The sequences of qRT-PCR primers for the other genes and PCR conditions are described in our previous studies (Yokoi et al., 2012a, b).

RNAi

RNAi-mediated gene knockdown was done as described in our previous studies (Yokoi et al., 2012a, b). Briefly, T7 RNA polymerase promoter sequence-tagged cDNA generated by conventional PCR was used as a template for dsRNA synthesis with the MEGAscript RNAi Kit (Ambion). One hundred nanograms of dsRNA, typically in a volume of 33 nl, for each target gene was injected into day 0 pupae using Nanoject II. Pupae were examined 72 h later for knockdown efficiency or challenged with microbes. dsRNA with a partial *maltose binding protein E* (*malE*) sequence served as a negative control. The sequences of primer pairs used for the production of T7 RNA polymerase promoter sequence (5'-TAATACGACTCACTATAGGG-3')-tagged cDNA is shown in Supplementary Table 1. The sequences of primer pairs used for *IMD* and *malE* cDNA template preparation are described in Yokoi et al. (2012b).

Survival assay

Day 0 pupae were treated with dsRNA. Pupae were challenged 72 h after the dsRNA treatment with live *E. cloacae* (50 nl, A_{600} = 0.1) or *B. subtilis* (100 nl, A_{600} = 3.0), as described in Yokoi et al. (2012a). The survival of pupae was thereafter recorded every 24 h. Data were presented as Kaplan-Meier plots and *P*-values calculated using the Gehan-Breslow-Wilcoxon test by using a software package (Ekuseru-Toukei 2010 ver. 1.13, Social Survey Research Information Co., Ltd.).

Sequence analyses

Multiple amino acid sequence alignments were performed using Clustal Omega (version 1.2.4) (Sievers & Higgins, 2021). Newick files were constructed from Clustal Omega output files (aln files) using FastTree program version 2.1.10 (Price et al., 2009), and approximate maximum-likelihood phylogenetic trees constructed using newick files with MEGAX version 10.1.7 (Kumar et al., 2018). All sequence analyses were done with default settings. To search for functional domains in the *Caspar*, *DREDD* and *FADD* of *T. castaneum*, the predicted amino acid sequences of these genes were analysed using InterProScan with InterPro version 86.0 (Blum et al., 2021, URL: https://www.ebi.ac.uk/interpro/search/sequence/). All raw data from these analyses, which are fasta, aln, newick and gff files, are available in figshare (see Supplementary Data 1–3).

RESULTS

Phylogenetic analyses of Caspar, DREDD and FADD, and search for functional domains in *T. castaneum* Caspar, DREDD and FADD

The sequences of *T. castaneum* orthologues for *Caspar*, *DREDD* and *FADD* (Tc-Caspar, Tc-DREDD, and Tc-FADD, respectively) were obtained from gene set data based on *T. castaneum* genome data (Zou et al., 2007; Tribolium Genome Sequencing Consortium, 2008), and their deduced amino acid sequences were subjected to phylogenetic analyses (Supplementary Fig. 1) together with the related sequences of other organisms [*Aedes aegypti* (Linnaeus), *Anopheles gambiae* (Giles), *D. melanogaster*, *Bombyx mori* (Linnaeus), *Apis mellifera* (Linnaeus), *Nilaparvata lugens* (Stål), mouse (Linnaeus) and human] (Supplementary Fig. 1). Furthermore, functional domains in the predicted amino acid sequences of Tc-Caspar, Tc-DREDD and Tc-FADD were searched for by InterProScan (Supplementary Fig. 2). Supplementary Fig. 1A shows the phylogenetic tree of Caspar-related proteins. Tc-Caspar forms a clade with *B. mori* Caspar (Bm-Caspar), indicating that Bm-Caspar is the closest protein to Tc-Caspar in the phylogenetic tree. The results of InterProScan showed that Tc-Caspar has functionally important domains, which are the FAF1_UBA domain (functions as a Fas-associated domain), ubiquitin-associated (UAS) domain and ubiquitin-like regulatory X domain (UBX) (Supplementary Fig. 2A). The death effecter domain-interacting domain (DEDID) is not predicted but the ubiquitin-like motif is predicted (IPR029071) (Chu et al., 1995; Park et al., 2004; Kim et al., 2006; He et al., 2013). However, the Ubiquitin-like motif is found in the Ras-binding domain, suggesting that this motif functions as DEDID (Nassar et al., 1995). Similar analyses were performed on DREDD/Caspase 8 proteins and FADD proteins (the FADD orthologue is not present in the *N. lugens* genome). In the phylogenetic trees of *DREDD* and *FADD*, Tc-DREDD is located near a clade including *D. melanogaster*, *A. aegypti* and *A. gambiae* DEREDDs (Supplementary Fig. 1B), while Tc-FADD is located in a clade comprising *D. melanogaster* and *B. mori* FADDs (Supplementary Fig. 1C). The results of domain searches in Tc-DREDD InterProScan showed that Tc-DREDD has two caspase domains and a single death effector domain (DED) (Supplementary Fig. 2B), which were previously reported in *D. melanogaster* DEREDD and shown to be functionally important (Luelier et al., 2000). Tc-FADD has a single death domain and another death domain in the homologous superfamily result, which might correspond to the death domain and death -interacting domains, respectively in *D. melanogaster* FADD (Supplementary Fig. 2C)

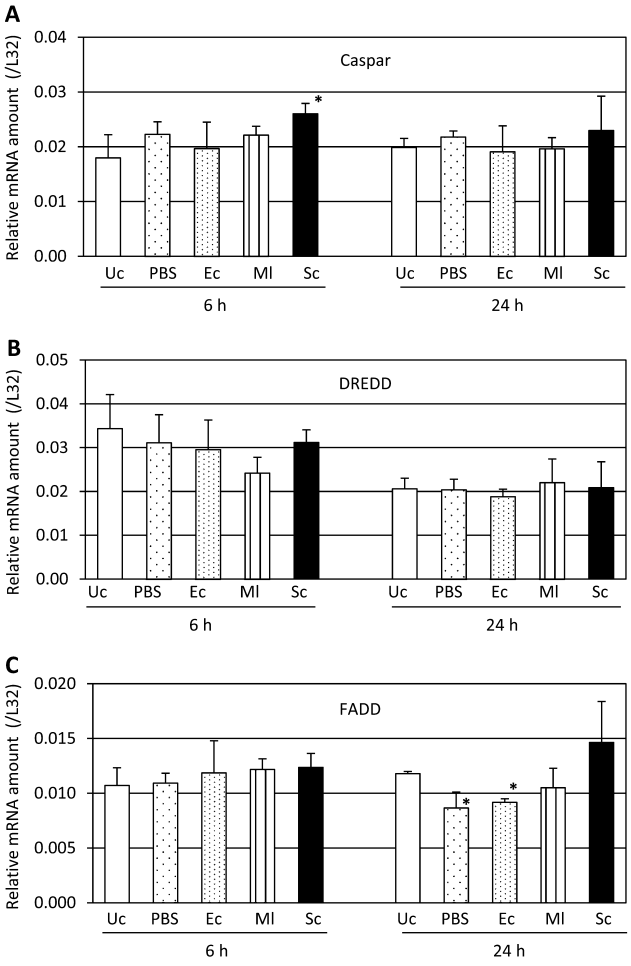

Fig. 1. Microbial challenge and effects on mRNA levels of *Caspar*, *DREDD* and *FADD*. Day 3 pupae were challenged with a heat-killed cell suspension of *E. coli* (Ec), *M. luteus* (Ml) or *S. cerevisiae* (Sc) and the mRNA levels of *Caspar* (A), *DREDD* (B) and *FADD* (C) were assessed using qRT-PCR, 6 and 24 h after a challenge. Unchallenged (Uc) and PBS-injected day 3 pupae (PBS) served as controls. mRNA values are shown relative to *RpL32* levels in the same samples. Experiments were independently carried out at least three times with 3 to 4 animals, and each column represents the mean ± S.D. Asterisks indicate a significant difference ($P < 0.05$ based on Student's *t*-tests) from the corresponding Uc controls.

(Hu & Yang, 2000). These results suggest that *Caspar*, *DREDD* and *FADD* in *T. castaneum* encode the functional counterparts of proteins in other species.

Microbial induction of *Caspar*, *DREDD and FADD*

The levels of expression of insect immune-related genes are frequently influenced by microbial invasion in several organisms, such as, *D. melanogaster* and *T. castaneum* (De Gregorio et al., 2001, 2002; Yokoi et al., 2012a, b). To confirm these findings, we investigated whether *T. castaneum Caspar*, *DREDD* and *FADD* were induced by an injection of heat-killed microbes (Fig. 1). The results indicate that the mRNA amounts of *Caspar* (Fig. 1A), *DREDD* (Fig. 1B) and *FADD* (Fig. 1C) were not or only weakly affected 6 and 24 h after the challenges with *E. coli*, *M. luteus* and *S. cerevisiae*.

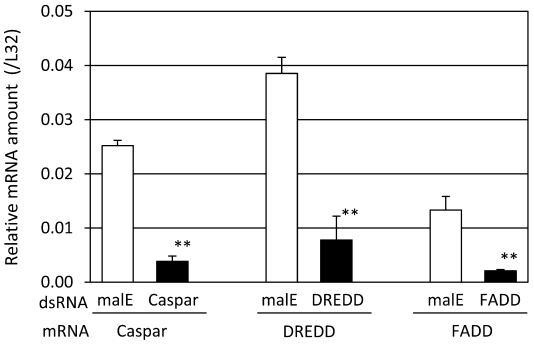

Fig. 2. Efficiency evaluation of RNAi-mediated gene knockdown. Day 0 pupa were injected with 100 ng of *Caspar*, *DREDD*, *FADD* or control *malE* dsRNA, and the levels of mRNA relative to those of *RpL32* were measured 72 h later. Experiments were independently carried out at least three times, and the mean ± S.D is shown. Double asterisks indicate $P < 0.01$ versus controls based on Student's *t*-test.

Efficiency of the injection of dsRNA in the knockdown of *Caspar*, *DREDD* and *FADD*

Prior to the functional assay of these three genes, we determined whether they were effectively knockdown by RNAi. Day 0 pupae were injected with the dsRNA for the respective targets along with control *malE* dsRNA and the amounts of mRNA were measured 72 h later. The results are presented in Fig. 2, which show that gene knockdown resulted in 80 to 85% reductions in the amounts of mRNA for all three genes.

Effects of the knockdown of *Caspar*, *DREDD* and *FADD* on the microbial induction of group I AMP genes

Using *Caspar*, *DREDD* and *FADD* knockdown pupae, the effects of the knockdown of these genes on the expressions of the group I genes, *Att1* (Fig. 3) and *Col1* (Fig. 4), are largely dependent on the IMD pathway (Yokoi et al., 2012b). Knockdown pupae and pupae treated with *malE* dsRNA as controls were challenged with the heat-killed cells of *E. coli*, *M. luteus* or *S. cerevisiae*, and the levels of mRNA in these treated pupae were measured 6 and 24 h after the challenges. As previously reported the amounts of *Att1* and *Col1* mRNA in unchallenged pupae were approximately 0.01 and 0.05 respectively (Yokoi et al., 2012a), which are clearly lower than those in *malE* dsRNA-treated control pupae, 6 and 24 h, post challenge with three microbes, except for *Att1* and *Col1* post challenge 24 h by *S. cerevisiae*. Thus, the results in Figs 3 and 4 can be considered to show the effects of the knockdown of *Caspar*, *DREDD* and *FADD* on *Col1* inductions by the three microbial challenges, except for Fig. 4F. The mRNA amounts of *Att1* in *DREDD*, *FADD* and *Caspar* dsRNA pre-treated pupae 6 h after the *E. coli* challenge were not significantly different from those in control pupae, whereas they were significantly lower in *DREDD* and *FADD* knockdown pupae than in control pupae 24 h after a challenge (Fig. 3A and 3B). Pupae treated with *Caspar* dsRNA, 6 and 24 h after the *E. coli* challenge had slightly higher mRNA amounts of *Att1* than control pupae. Comparisons

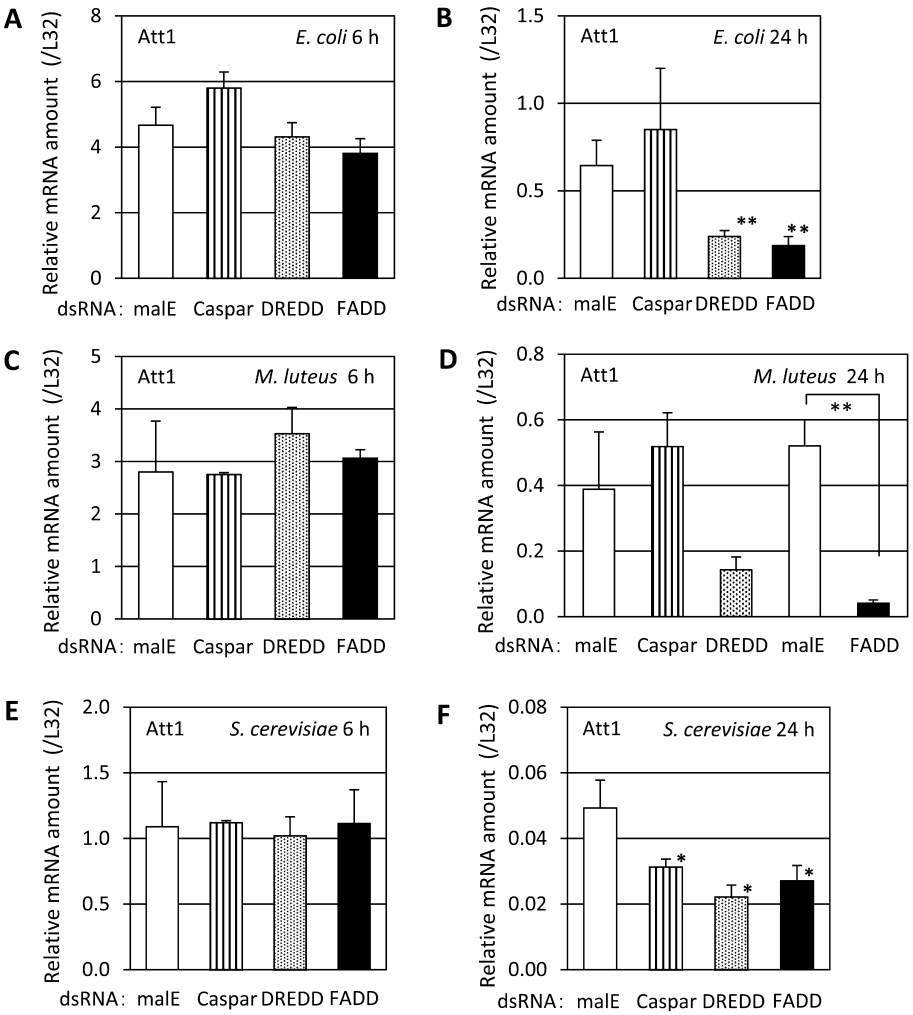

Fig. 3. Effects of the knockdown of *Caspar*, *DREDD* and *FADD* on the expression of the group I AMP gene, *Att1,* in pupae challenged by a microbe. Day 0 pupae were injected with a preparation of dsRNA. Seventy-two hours later, the dsRNA-treated pupae were injected with a heat-killed cell suspension of *E. coli* (A and B), *M. luteus* (C and D) or *S. cerevisiae* (E and F). The relative levels of mRNA of *Att1* to *RpL32* were assessed 6 (A, C and E) and 24 h (B, D and E) after the microbial challenge and are shown as the mean ± S.D. Experiments were independently repeated at least three times with three animals each. Single asterisks indicate $P < 0.05$ versus *malE* controls based on Student's *t*-tests, while double asterisks denote $P < 0.01$.

of the mRNA amounts of *Att1* in control pupae challenged with *E. coli* and *M. luteu*s revealed that the levels of activation of *Att1* induced by the *M. luteus* challenge were lower than those of the *E. coli* challenge, which is consistent with previous findings (Yokoi et al., 2012a). The effects of the knockdown of *DREDD*, *FADD*, or *Caspar* on gene induction did not significantly alter the levels of *Att1* mRNA 6 h after the *M. luteus* challenge (Fig. 3C). Pupae treated with *DREDD* or *FADD* dsRNA had lower mRNA levels of *Att1* 24 h after the *M. luteus* challenge than control pupae (*Att1* mRNA levels of DREDD knockdown and control pupae were clearly different but not significantly so), while the pupae with *Caspar* dsRNA showed modest enhancements 24 h after the *M. luteus* challenge (Fig. 3D). Six hours after the *S. cerevisiae* challenge, no significant differences were observed in *Att1* mRNA levels between any dsRNA-treated and control pupae (Fig. 3E). Significantly lower mRNA levels of *Att1* 24 h after the *S. cerevisiae* challenge were recorded in *DREDD*, *FADD* and *Caspar* dsRNA-treated pupae than in control pupae (Fig. 3F).

Similar knockdown and microbial induction experiments were performed for the group I gene, *Col1* (Fig. 4). Overall results were similar to those for *Att1*. Six hours after the *E. coli* challenge, *Col1* mRNA amounts were significantly lower in *DREDD* knockdown pupae than in control pupae, but did not differ significantly between *FADD* knockdown and control pupae (Fig. 4A). *Col1* mRNA amounts were significantly higher in *Caspar* knockdown pupae than in control pupae. Twenty-four hours after the *E. coli* challenge, *Col1* mRNA amounts were significantly lower in *DREDD* and *FADD* knockdown pupae than in control pupae, while those in *Caspar* knockdown pupae were slightly higher (Fig. 4B). *Col1* mRNA amounts in *DREDD*, *FADD* and *Caspar* knockdown pupae 6 h after the *M. luteus* challenge did not differ significantly from those in the control pupae (Fig. 4C). Twenty-four hours after the *M. luteus* challenge, *Col1* mRNA amounts were slightly higher and lower in *Caspar* and *DREDD* knockdown pupae, respectively, than in control pupae, but were significantly lower in *FADD* knockdown pupae than in

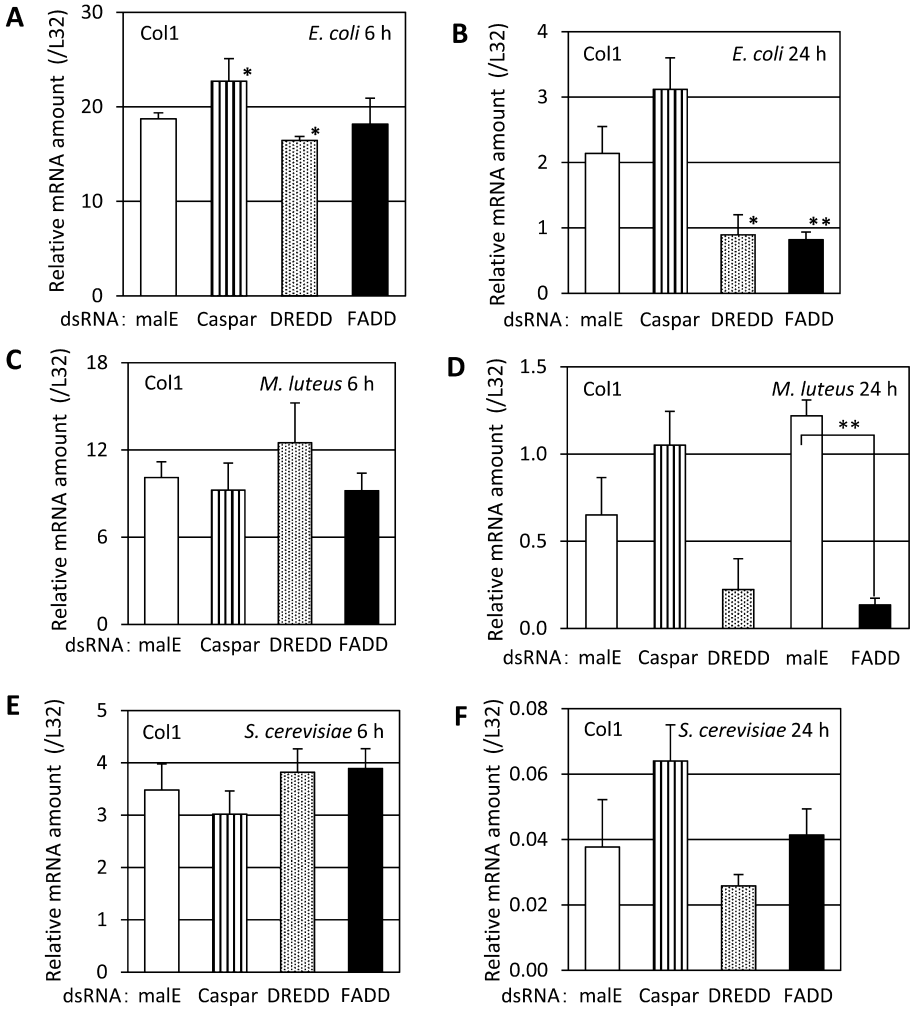

Fig. 4. Effects of the knockdown of *Caspar*, *DREDD* and *FADD* on the expression of the group I AMP gene, *Col1,* in pupae challenged by a microbe. Day 0 pupae were injected with preparations of dsRNA. Seventy-two hours later, the dsRNA-treated pupae were injected with a heat-killed cell suspension of *E. coli* (A and B), *M. luteus* (C and D) or *S. cerevisiae* (E and F). The relative levels of mRNA of *Att1* to *RpL32* were assessed 6 (A, C and E) and 24 h (B, D and E) after a microbial challenge and shown as the mean ± S.D. Experiments were independently repeated at least three times with three animals each. Single asterisks indicate $P < 0.05$ versus *malE* controls based on Student's *t*-tests, while double asterisks denote $P < 0.01$.

control pupae (Fig. 4D). Similar to 6 h after the *M. luteus* challenge, no significant differences were recorded in *Col1* mRNA amounts between *DREDD*, *FADD* and *Caspar* knockdown pupae and control pupae 6 h after the *S. cerevisiae* challenge (Fig. 4E). *Col1* mRNA amounts varied among *DREDD*, *FADD* and *Caspar* knockdown pupae and control pupae 24 h after the *S. cerevisiae* challenge, but were not significantly different (Fig. 4F).

Effects of the knockdown of *Caspar*, *DREDD* and *FADD* on the microbial induction of the group II AMP gene

The results recorded for the group II gene *Def3* were distinct from those for group I genes (Fig. 5). The level of expression of *Def3* in unchallenged pupae is approximately 0.003 (Yokoi et al., 2012a), which is clearly a lower value than that recorded in pupae treated with *malE* dsRNA and post challenged 6 and 24 h later with three microbes, except for post challenge 24 h with *M. luteus* and *S. cerevisiae*. Thus, results in Fig. 5A, B, C and E are considered to show effects of the knockdown of *Caspar*, *DREDD* and *FADD* on *Def3* inductions by the three microbial challenges. Levels of *Def3* expression 6 h after the *E. coli* challenge were significantly lower in *DREDD* knockdown pupae than in control pupae, while those in *Caspar* knockdown pupae were significantly higher (Fig. 5A). Levels of expression of *Def3* were slightly lower in *FADD* knockdown pupae. Similar results were obtained for pupae 24 h after the *E. coli* challenge (Fig. 5B). Levels of expression of *Def3* were similar in pupae 6 h after the *M. luteus* and *E. coli* challenges, with the lack of significant differences attributed to large variations in *malE* control values (Fig. 5C). Twenty-four hours after the *M. luteus* challenge, the levels of expression of *Def3* were significantly lower in *DREDD* and *FADD* knockdown pupae than in control pupae, but were higher in *Caspar* knockdown pupae (Fig. 5D). Regarding the induction by *S. cerevisiae* 6 h after the challenge, the knockdown of *DREDD* and *FADD* appeared to suppress the induction of *Def3* (Fig. 5E). The induction profiles of *Def3* by *M. luteus* and *S. cerevisiae* at 24 h post challenge

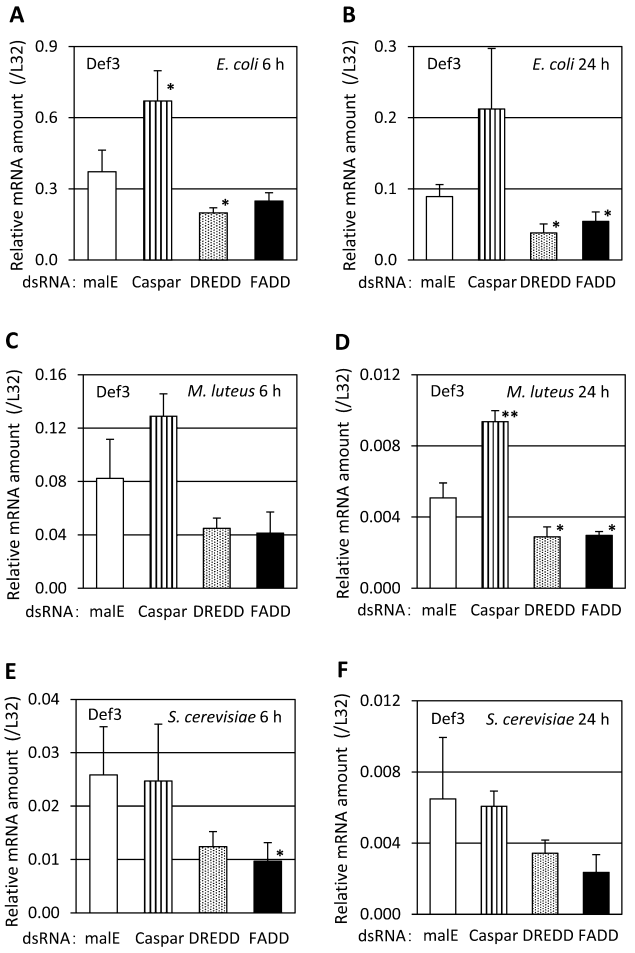

Fig. 5. Effects of the knockdown of *Caspar*, *DREDD* and *FADD* on the expressions of the group II AMP gene, *Def3,* in pupae challenged by a microbe. Day 0 pupae were injected with preparations of dsRNA. Seventy-two hours later, the dsRNA-treated pupae were injected with a heat-killed cell suspension of *E. coli* (A and B), *M. luteus* (C and D) or *S. cerevisiae* (E and F). The relative levels of mRNA of *Att1* to *RpL32* were assessed 6 (A, C and E) and 24 h (B, D and F) after the microbial challenge and shown as the mean ± S.D. Experiments were independently repeated at least three times with three animals each. Single asterisks indicate $P < 0.05$ versus *malE* controls based on Student's *t*-tests.

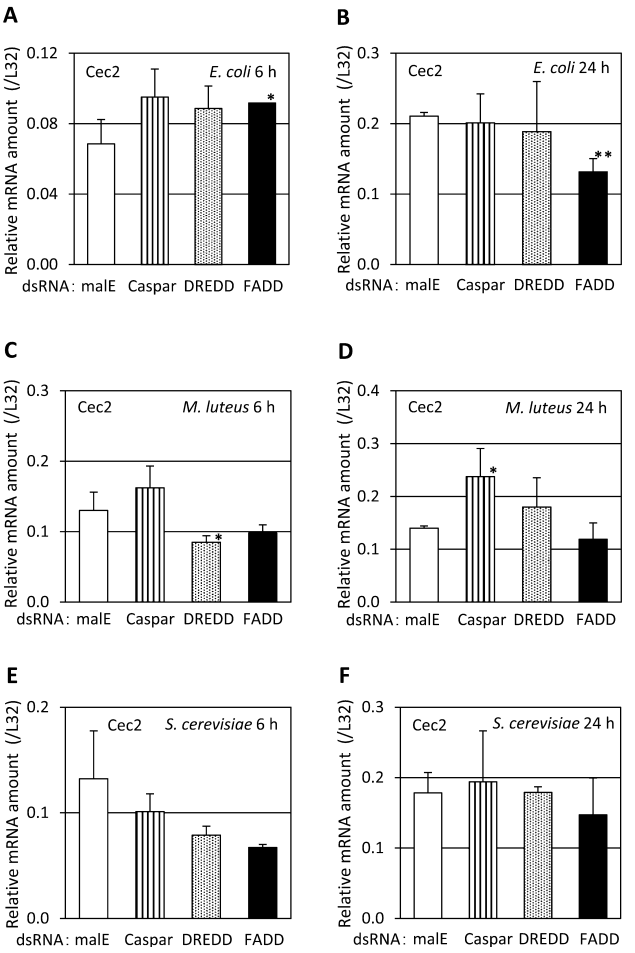

Fig. 6. Effects of the knockdown of *Caspar*, *DREDD* and *FADD* on the expression of the group III AMP gene, *Cec2,* in pupae challenged by a microbe. Day 0 pupae were injected with preparations of dsRNA. Seventy-two hours later, the dsRNA-treated pupae were injected with a heat-killed cell suspension of *E. coli* (A and B), *M. luteus* (C and D) or *S. cerevisiae* (E and F). The relative levels of mRNA of *Att1* to *RpL32* were assessed 6 (A, C and E) and 24 h (B, D and F) after a microbial challenge and shown as the mean ± S.D. Experiments were independently repeated at least three times with three animals each. Single asterisks indicate $P < 0.05$ versus *malE* controls based on Student's *t*-tests.

apparently exhibits some knockdown effects, but in both cases the induction will have ceased by this time according to our previous results (Yokoi et al., 2012a, b) and is well supported by the low *Def3* mRNA levels (Fig. 5D and 5F).

Effects of the knockdown of *Caspar*, *DREDD* and *FADD* on the microbial induction of group III AMP genes

Two group III genes, *Cec2* and *Cec3*, the expression of which is largely dependent on Toll signaling, were investigated (Figs 6 and 7) (Yokoi et al., 2012b). the values of the expressions of *Cec2* and *Cec3* in unchallenged pupae is approximately 0.02 and 0.1, respectively (Yokoi et al., 2012a, b), which are clearly lower than those recorded for *malE* dsRNA-treated controls depicted in Figs 6 and 7. Thus, the results in Figs 6 and 7 can be considered to show the effects of the knockdown of *Caspar*, *DREDD* and *FADD* on the induction of *Cec2* and *Cec3*, respectively, by the three microbial challenges. The level of expression of *Cec2* in *Caspar* and *DREDD* knockdown pupae 6 h after the challenge with *E. coli* did not differ significantly from those in control pupae, while modest up-regulation and suppression were only recorded in *FADD* knockdown pupae 6 and 24 h, respectively, after the challenge (Fig. 6A and 6B). Six hours after the challenge with *M. luteus*, the amounts of *Cec2* mRNA were significantly and slightly lower in *DREDD* and *FADD* knockdown pupae, respectively, than in control pupae (Fig. 6C). Twenty-four hours after the challenge, the amounts of *Cec2* mRNA in *DREDD* and *FADD* knockdown pupae did not differ significantly from those in control pupae (Fig. 6D). The knockdown of *Caspar* appeared to activate effects that became more prominent (also significantly different) in the later phase of induction (Fig. 6C and 6D). No significant differences were recorded between *Caspar*, *DREDD* and *FADD* knockdown

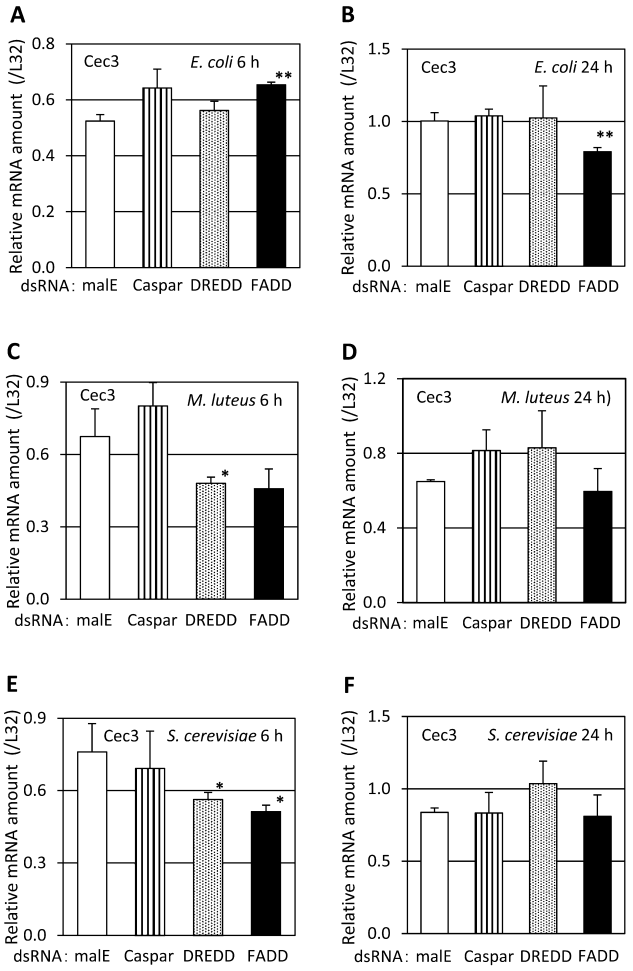

Fig. 7. Effects of the knockdown of *Caspar*, *DREDD* and *FADD* on the expression of the group III AMP gene, *Cec3,* in pupae challenged by a microbe. Day 0 pupae were injected with preparations of dsRNA. Seventy-two hours later, the dsRNA-treated pupae were injected with a heat-killed cell suspension of *E. coli* (A and B), *M. luteus* (C and D) or *S. cerevisiae* (E and F). The relative levels of mRNA of *Att1* to *RpL32* were assessed 6 (A, C and E) and 24 h (B, D and F) after a microbial challenge and shown as the mean ± S.D. Experiments were independently repeated at least three times with three animals each. Single asterisks indicate $P < 0.05$ versus *malE* controls based on Student's *t*-tests.

pupae and control pupae 6 or 24 h after the challenge with *S. cerevisiae* (Fig. 6E and 6F).

Levels of expression of *Cec3* 6 h after the challenge with *E. coli* were slightly higher in *Caspar* and *FADD* knockdown pupae than in control pupae, but were similar in DREDD knockdown pupae and control pupae (Fig. 7A). Twenty-four hours after the challenge, the levels of expression of *Cec3* were slightly lower in *FADD* knockdown pupae than in control pupae, while there was no difference of the levels of *Cec3* expression between *Caspar* or *FADD* knockdown and control pupae (Fig. 7B). Six hours after the challenge with *M. luteus*, amounts of *Cec3* mRNA in *DREDD* and *FADD* knockdown pupae were less than in the controls (Fig. 7C). Amounts of *Cec3* 6 h after the challenge with *M. luteus* were slightly more abundant in *Caspar* knockdown pupae. Twenty-four hours after the *M. luteus* challenge, no significant differences were recorded in the amounts of *Cec3* mRNA in *Caspar*, *DREDD* and *FADD* knockdown pupae and control pupae (Fig. 7D). Furthermore, amounts of *Cec3* mRNA did not differ significantly in *Caspar* knockdown and control pupae 6 or 24 h after the challenge with *S. cerevisiae* (Fig. 7E and 7F). Levels of expression of *Cec3* 6 h after the challenge with *S. cerevisiae* were lower in *DREDD* and *FADD* knockdown pupae than in control pupae, while no significant differences were recorded 24 h after the challenge (Fig. 7E and 7F).

Survival assays

To clarify the involvement of these IMD pathway-associated intracellular factors in the antimicrobial host defenses of *T. castaneum*, survival was assayed using two model pathogenic bacterial strains. Pupae pre-treated with dsRNA were inoculated intrahaemocoelically with defined doses of live *E. cloacae* or *B. subtilis*, and percentage survival was then recorded every 24 h. *malE* dsRNA-treated pupae served as negative controls, while those treated with *IMD* dsRNA were positive controls. Results are shown in Kaplan-Meier plots (Fig. 8). In comparisons with the negative control, the knockdown of *IMD* severely impaired host defenses against *E. cloacae* and *B. subtilis* (Fig. 8A to 8D). *DREDD* and *FADD* knockdown pupae represented intermediate phenotypes. The knockdown of *FADD* had similar effects to that of *IMD* in terms of defense against the two bacteria, while those of the knockdown of *DREDD* appeared to be weaker. *DREDD* knockdown pupae succumbed to *E. cloacae* infection slightly faster than *malE* controls ($P = 0.0536$, Fig. 8B). In addition, the knockdown of *DREDD* significantly weakened host defense against *B. subtilis,* and the *P*-value was higher than in the case of *IMD* knockdown (Fig. 8D). The knockdown of *Caspar* resulted in slightly higher levels of mRNA of some AMP genes than in the *malE* control (Figs 3 to 7). Nevertheless, it did not increase the resistance to these two bacterial pathogens.

DISCUSSION

In the present study, we examined the genes coding for potential receptor-proximal components of the IMD pathway in the model beetle *T. castaneum*, namely, *Caspar*, *DREDD* and *FADD*, the products of which are constituents of the IMD pathway of *Drosophila* (Kleino & Silverman, 2014). We previously reported that the IMD and Toll pathways of *T. castaneum* exhibit a nearly non-specific manner of activation in terms of microbial species used as an elicitor, while the magnitude of activation differed depending on the type of microbe (Yokoi et al., 2012a, b). In the present study, we investigated the involvement of these genes in the activation of this indiscriminate immune pathway, which indicates a marked difference in the immune signaling in this model beetle from the *Drosophila* system.

Caspar, *DREDD* and *FADD* in *T. castaneum* encode proteins bearing structural features that are typical of the respective family members, including domain configurations, suggesting that these are orthologous genes of the functionally defined counterparts in other organisms. We then showed that these genes were not activated by im-

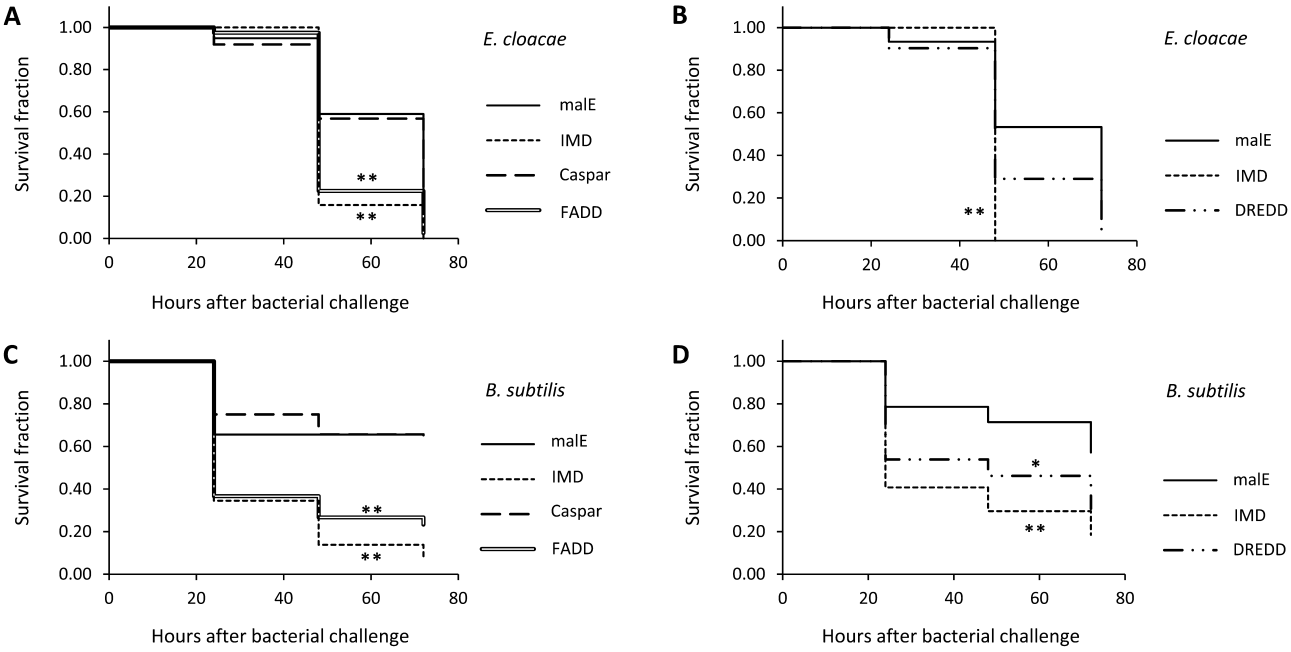

Fig. 8. Effects of the knockdown of *Caspar*, *DREDD* and *FADD* on host defensees against two model bacterial pathogens. Day 3 pupae that were treated with respective preparations of dsRNA on day 0 were challenged by either *E. cloacae* (A and B) or *B. subtilis* (C and D), and the survival of pupae thereafter was monitored and recorded every 24 h. Results are shown in Kaplan-Meier plots. The first set of experiments was carried out using *malE*, *IMD*, *Caspar* and *FADD* dsRNA-treated pupae (A and C), and the second set using *malE*, *IMD*,and *DREDD* dsRNA-treated pupae (B and D). *malE* dsRNA served as negative controls, while *IMD* dsRNA provided positive controls. Significant differences from *malE*-treated controls based on the Gehan-Breslow-Wilcoxon test are denoted by * ($P < 0.05$) or ** ($P < 0.01$).

mune challenges with *E. coli*, *M. luteus* or *S. cerevisiae*. We characterized these genes by estimating their contribution to the microbial induction of two group I genes that represent the IMD pathway read-out. While the results obtained 6 h after the microbial challenge were obscure, the knockdown of *DREDD* and *FADD* resulted in the unequivocal suppression of these two IMD pathway-dependent genes after 24 h. Based on these results, we conclude that *DREDD* and *FADD* functioned as canonical constituents of the IMD pathway in this beetle. We previously conducted similar experiments that targeted *IMD*, and found that the knockdown of *IMD* took effect by 6 h after the microbial challenge, with an approximately 50% reduction in group I gene induction (Yokoi et al., 2012b). Based on similar reductions in the mRNA levels of these factors upon the dsRNA treatment in our present and previous studies, the different phenotypes in the earlier phase of microbial gene induction may be ascribed to the different half-lives of the corresponding proteins. Alternatively, since *DREDD* encodes the proteolytic enzyme that may process more downstream substrates (Stöven et al., 2000), IMD signaling may be less sensitive to reductions in the amount of the DREDD protein than that of the IMD protein, which provides a molecular scaffold for pathway activation. Moreover, when we assume that the adaptor protein FADD is functioning through its binding to the DREDD protein, the knockdown of *FADD* showing similar phenotypes to those with the knockdown of *DREDD* appears to be reasonable (Kleino & Silverman, 2014). In addition to these assumptions, we cannot rule out the existence of unidentified genes that provide some functional redundancy to *DREDD* or *FADD*. These knockdown phenotypes of *DREDD* and *FADD*, and previously obtained IMD knockdown phenotypes in terms of group I gene induction, along with the results of group II and group III genes, appear to be consistent with the results of the survival assays in the present study with the following order of severe impairments in host defenses: *IMD* knockdown ≥ *FADD* knockdown > *DREDD* knockdown.

We noted that the early-phase responses of the group I genes *Att1* and *Col1* appeared to be slightly more sensitive to the gene knockdown of these intracellular factors when challenged with *E. coli* than with *M. luteus*. In terms of group I gene induction, *E. coli* is approximately 1.5-fold to 4-fold more potent than *M. luteus* (the present study, Yokoi et al., 2012b, a). The double knockdown of PGRP-LA plus PGRP-LC, PGRP-LD, or PGRP-LE or the triple knockdown of the PGRP-LA, PGRP-LC and PGRP-LE proteins, however, suppress the induction of group I and II AMP genes by an *E. coli* or *M. luteus* challenge. These findings indicate that PGRP-LA bound by an *E. coli*-derived DAP-type peptidoglycan or *M. luteus*-derived Lys-type peptidoglycan undergo strong conformational changes that intensively recruit intracellular components, suggesting the lack of a clear difference in the strength of the recognition of both types of peptidoglycans (Koyama et al., 2015). Differences in sensitivities to reductions in group I AMP genes may be attributed to differences in signal strengths, which activate the IMD and Toll pathways during the *E. coli* and *M. luteus* challenges; *M. luteus* may activate the Toll pathway more strongly than *E. coli.*

Group I gene induction by heat-killed *S. cerevisiae* 6 h after the challenge was not affected by the knockdown of

Caspar, *DREDD* or *FADD*. Twenty-four hours after the challenge, mRNA levels of *Att1* in *Caspar*, *DREDD* and *FADD* knockdown pupae were lower than in control pupae, while *Col1* expression was not affected by any of the three knockdowns. The induction of group I genes, including *Att1* by heat-killed *S. cerevisiae* cells, has ceased by this time (Yokoi et al., 2012a). Actually, *Att1* mRNA levels in control pupae 24 h post challenges (approximately 0.05 in Fig. 3F) were not so different from in unchallenged pupae (approximately 0.01 (Yokoi et al., 2012a)) compared to that in the other conditioned pupae. (*Att1* levels in control pupae 24h post *E. coli* and *M. luteus* challenges was approximately 0.6 and 0.4 respectively). These results indicate that the observed differences reflect variations in the status of the final phase. Furthermore, based on these results, we conclude that *DREDD* and *FADD* constitute the canonical IMD pathway of *T. castaneum*, as in *Drosophila*, and are not mainly involved in immune signaling induced by the *S. cerevisiae* challenge. Regarding Caspar, its inhibitory effects on the activation of the IMD pathway appeared to be weak or negative and counteracted DREDD in some cases.

The kinetics of group II gene *Def3* differed from those of the group I gene upon gene knockdown of these intracellular factors. The suppressive effects of the knockdown of *DREDD* and *FADD* became apparent 6 h after an *E. coli* or *M. luteus* challenge. These results indicate that the group II gene is more sensitive to a decrease in IMD pathway components than group I genes, which is consistent with our previous findings on *IMD* (Yokoi et al., 2012b) *PGRP-LA* (Koyama et al., 2015). As described above, PGRP-LA functions as the canonical receptor of the *T. castaneum* IMD pathway, and this isoform recognizes Gram-negative DAP-type peptidoglycans and Gram-positive Lys-type peptidoglycans. In addition, analyses of the 3' regions of these AMP genes reveal that each group I gene has a single copy of the κB motif potentially bound by Relish, while group II *Def3* has two inverted copies of potential κB motifs (Yokoi et al., 2012a). Collectively, these findings indicate that the expression of group I genes is readily driven by one Relish molecule, while other classes of transcription factors, such as tissue- or developmental stage-specific factors, synergistically support their high levels of expression (Rus et al., 2013). On the other hand, the full activation of group II *Def3* may at least require the occupation of two copies of κB sites in its proximal promoter region by two molecules of the activated Relish protein. These findings account for the nature of *Def3*, in that it responds more sensitively to the decline in IMD pathway constituents. The degree of *Def3* suppression upon knockdown of *DREDD* and *FADD* 24 h after the *E. coli* challenge appeared to be less conspicuous than those for group I genes and the results of the *M. luteus* or *S. cerevisiae* challenge after 24 h was not considered because the induction of *Def3* had ceased before then and also because lower levels of expression of *Def3* were recorded in control pupae post challenge 24 h with *M. luteus* and *S. cerevisiae* than in the conditioned pupae as described in the previous paragraph (Yokoi et al., 2012a). This finding may be attributed to the Toll pathway-dependent nature of *Def3*, which supports the later phase of the induction of *Def3*.

The group III genes, *Cec2* and *Cec3,* are largely dependent on the Toll pathway for their microbial induction (Yokoi et al., 2012a, b). We determined the involvement of *DREDD* and *FADD* in group III gene regulation and found that the knockdown of *DREDD* significantly suppressed gene induction 6 h after the *M. luteus* challenge, while the effects of the knockdown of *FADD* in terms of the suppression of induction by *E. coli* were recorded 24 h after the challenge. Since this was the case for *Cec2* and *Cec3*, it is reasonable to speculate that these factors function at points common to the regulatory cascade of these group III genes, namely, the Toll pathway, and not due to a decrease in the terminal NF-κB transcription factor of the IMD pathway, Relish. The low sensitivity of group III genes to the knockdown of Relish provides support for this idea (Yokoi et al., 2012a). Six hours after the *M. luteus* challenge, the knockdown of *FADD* had a similar outcome to that of *DREDD* on the induction of both *Cec2* and *Cec3*, indicating that these two Toll-dependent group III genes are also regulated by *FADD* and *DREDD* via common mechanisms and that the products of these two genes cooperate in this putative path similar to the multimeric molecular assembly activation of the IMD pathway (Kleino & Silverman, 2014). Since the knockdown of *IMD* did not suppress the induction of the group III gene by *M. luteus* after 6 h (Yokoi et al., 2012b), DREDD and FADD appear to function independently of the IMD protein under these conditions. Twenty-four hours after the *E. coli* challenge, the knockdown of DREDD and FADD resulted in distinct phenotypes; only the knockdown of *FADD* negatively affected the induction of the group III gene. This result indicates that the FADD protein has different roles under these two distinct conditions.

Caspar was initially identified as a suppressor of IMD signaling based on the genetic screening of a set of *Drosophila* mutants (Kim et al., 2006). Caspar, which is homologous to mammalian Fas-associating factor 1 (Chu et al., 1995), targets the proteolytic activation of Relish by DREDD. Its loss-of-function phenotype involves the constitutive expression of AMP genes associated with the IMD pathway and increased resistance to Gram-negative infection. In the present study on *T. castaneum*, the knockdown of *Caspar* generally resulted in an opposite effect on the induction of the microbial AMP gene when that of *DREDD* had a negative effect. This result appears to support the functions of DREDD recorded in the present study, which depends on its caspase activity. The basal levels of mRNA of AMP genes were not elevated in unchallenged *Caspar* knockdown pupae (data not shown). This result, taken together with the mild phenotypes of challenged *Caspar* knockdown pupae for the induction of the AMP gene, appear to be consistent with the results of survival assays showing that the knockdown of *Caspar* did not increase the percentage survival over that of *malE*-treated controls.

Of the three microbes used as elicitors in the present study, we did not obtain clear results with *S. cerevisiae*.

The transcriptional activation of *T. castaneum* AMP genes by *S. cerevisiae* is very dependent on Toll signaling, even for group I genes (Yokoi et al., 2012b), and in a subsequent study on NF-κB transcription factor genes involved in the immune challenge from *S. cerevisiae* they may evoke unidentified activating signals other than IMD or Toll signaling (Yokoi et al., 2012a). Therefore, we attribute the equivocal results obtained with *S. cerevisiae* in the present study to the nature of *S. cerevisiae* as an elicitor.

We compared the immune reactions related to IMD, Toll pathway and induction of the AMP gene with our results on *T. castaneum* and previous findings on *D. melanogaster*. Data recorded for *T. castaneum* were from pupae, whereas those for *D. melanogaster* were mainly for adult flies. In *D. melanogaster*, the induction levels of several AMP genes, including *Dipetericin, CecropinA, Drosocin* and *AttacinA*, differ in third instar larvae and adults (Verma & Tapadia, 2012). Therefore, the levels of induction of AMP may differ between pupae and other life stages in *T. castaneum*. Moreover, comparison of the present results for *T. castaneum* pupae with previous findings on *Drosophila,* which were mainly obtained from adults, may be inappropriate. Although the levels of induction of AMP may differ between life stages, both in *D. melanogaster* and *T. castaneum*, the basic immune regulation of AMP genes by Toll and IMD pathways did not markedly differ between the life stages. Therefore, a discussion on the differences in immune signaling via the Toll and IMD pathways between *T. castameum* and *D. melanogaster* based on comparisons of the present results with previous findings on *D. melanogaster,* as described above, is appropriate for the interpretation of immune signaling.

In the present study, we determined the involvement of the *Caspar*, *DREDD* and *FADD* genes of *T. castaneum* in two immune signaling pathways, namely, the IMD and Toll pathways. The results indicate that the intracellular factors encoded by these genes represented the canonical constituents of the IMD pathway in this beetle, as in *Drosophila*. Furthermore, the present study demonstrated that DREDD and FADD influenced the activation of Toll-dependent group III AMP genes, presumably through their IMD-independent functions to some extent. This intracellular component shared by the two immune signaling pathways provides possible points of signal crosstalk between the two pathways and will facilitate further research on the molecular background of the indiscriminate microbial pathway activation characteristics of *T. castaneum's* antimicrobial immunity.

ACKNOWLEDGEMENTS. This work was supported by JSPS KAKENHI Grant Numbers JP21H03831 to K. Yokoi and 20K06050 to K. Miura. We also thank Y. Yagi, T. Ushimaru, A. Miyanoshita, and M. Murata for providing research material.

REFERENCES

Blum M., Chang H.Y., Chuguransky S., Grego T., Kandasaamy S., Mitchell A., Nuka G., Lafosse-Paysan T. et al. 2021: The InterPro protein families and domains database: 20 years on. — *Nucleic Acids. Res.* **49**(D1): D344–D354.

Choe K.M., Werner T., Stoven S., Hultmark D. & Anderson K.V. 2002: Requirement for a peptidoglycan recognition protein (PGRP) in relish activation and antibacterial immune responses in *Drosophila*. — *Science* **296**: 359–362.

Choe K.M., Lee H. & Anderson K.V. 2005: *Drosophila* peptidoglycan recognition protein LC (PGRP-LC) acts as a signal-transducing innate immune receptor. — *Proc. Natl. Acad. Sci. U.S.A.* **102**: 1122–1126.

Chu K., Niu X. & Williams L.T. 1995: A Fas-associated protein factor, FAF1, potentiates Fas-mediated apoptosis. — *Proc. Natl. Acad. Sci. U.S.A.* **92**: 11894–11898.

De Gregorio E., Spellman P.T., Rubin G.M. & Lemaitre B. 2001: Genome-wide analysis of the *Drosophila* immune response by using oligonucleotide microarrays. — *Proc. Natl. Acad. Sci. U.S.A.* **98**: 12590–12595.

De Gregorio E., Spellman P.T., Tzou P., Rubin G.M. & Lemaitre B. 2002: The Toll and Imd pathways are the major regulators of the immune response in *Drosophila*. — *EMBO J.* **21**: 2568–2579.

Ferrandon D., Imler J.-L., Hetru C. & Hoffmann J.A. 2007: The *Drosophila* systemic immune response: sensing and signaling during bacterial and fungal infections. — *Nat. Rev. Immunol.* **7**: 862–874.

Gangloff M., Murali A., Xiong J., Arnot C.J., Weber A.N., Sandercock A.M., Robinson C.V., Sarisky R. et al. 2008: Structural insight into the mechanism of activation of the Toll receptor by the dimeric ligand Spätzle. — *J. Biol. Chem.* **283**: 14629–14635.

Gobert V., Gottar M., Matskevich A.A., Rutschmann S., Royet J., Belvin M., Hoffmann J.A. & Ferrandon D. 2003: Dual activation of the *Drosophila* Toll pathway by two pattern recognition receptors. — *Science* **302**: 2126–2130.

Gottar M., Gobert V., Matskevich A.A., Reichhart J.-M., Wang C., Butt T.M., Belvin M., Hoffmann J.A. & Ferrandon D. 2006: Dual detection of fungal infections in *Drosophila* via recognition of glucans and sensing of virulence factors. — *Cell* **127**: 1425–1437.

Guntermann S. & Foley E. 2011: The protein Dredd is an essential component of the c-Jun N-terminal kinase pathway in the *Drosophila* immune response. — *J. Biol. Chem.* **286**: 30284–30294.

He Z., Wang P., Shi H., Si F., Hao Y. & Chen B. 2013: Fas-associated factor 1 plays a negative regulatory role in the antibacterial immunity of *Locusta migratoria*. — *Insect Mol. Biol.* **22**: 389–398.

Horng T. & Medzhitov R. 2001: *Drosophila* MyD88 is an adapter in the Toll signaling pathway. — *Proc. Natl. Acad. Sci. U.S.A.* **98**: 12654–12658.

Hu S. & Yang X. 2000: dFADD, a novel death domain-containing adapter protein for the *Drosophila* caspase DREDD. — *J. Biol. Chem.* **40**: 30761–30764.

Hultmark D. 2003: *Drosophila* immunity: paths and patterns. — *Curr. Opin. Immunol*. **15**: 12–19.

Kaneko T., Yano T., Aggarwal K., Lim J.H., Ueda K., Oshima Y., Peach C., Erturk-Hasdemir D. et al. 2006: PGRP-LC and PGRP-LE have essential yet distinct functions in the *Drosophila* immune response to monomeric DAP-type peptidoglycan. — *Nat. Immunol.* **7**: 715–723.

Kim M., Lee J.H., Lee S.Y., Kim E. & Chung J. 2006: *Caspar*, a suppressor of antibacterial immunity in *Drosophila*. — *Proc. Natl. Acad. Sci. U.S.A.* **103**: 16358–16363.

Kleino A. & Silverman N. 2014: The *Drosophila* IMD pathway in the activation of the humoral immune response. — *Dev. Comp. Immunol.* **42**: 25–35.

Koyama H., Kato D., Minakuchi C., Tanaka T., Yokoi K. & Miura K. 2015: Peptidoglycan recognition protein genes and their roles in the innate immune pathways of the red flour beetle, *Tribolium castaneum*. — *J. Invertebr. Pathol.* **132**: 86–100.

Kumar S., Stecher G., Li M., Knyaz C. & Tamura K. 2018: MEGA X: Molecular Evolutionary Genetics Analysis across computing platforms. — *Mol. Biol. Evol.* **35**: 1547–1549.

Lemaitre B. & Hoffmann J. 2007: The host defense of *Drosophila melanogaster*. — *Annu. Rev. Immunol.* **25**: 697–743.

Leulier F., Rodriguez A., Khush R.S., Abrams J.M. & Lemaitre B. 2000: The *Drosophila* caspase Dredd is required to resist Gram-negative bacterial infection. — *EMBO Rep.* **1**: 353–358.

Meinander A., Runchel C., Tenev T., Chen L., Kim C.H., Ribeiro P.S., Broemer M., Leulier F. et al. 2012: Ubiquitylation of the initiator caspase DREDD is required for innate immune signaling. — *EMBO J.* **31**: 2770–2783.

Naitza S., Rosse C., Kappler C., Georgel P., Belvin M., Gubb D., Camonis J., Hoffmann J.A. et al. 2002: The *Drosophila* immune defense against gram-negative infection requires the death protein dFADD. — *Immunity* **17**: 575–581.

Nassar N., Horn G., Herrmann C.A., Scherer A., McCormik F. & Wittingghofer A. 1995: The 2.2 Å crystal structure of the Ras-binding domain of the serine/threonine kinase c-Raf1 in complex with RaplA and a GTP analogue. — *Nature* **375**: 554–560.

Paquette N., Broemer M., Aggarwal K., Chen L., Husson M., Erturk-Hasdemir D., Reichhart J.-M., Meier P. et al. 2010: Caspase-mediated cleavage, IAP binding, and ubiquitination: Linking three mechanisms crucial for *Drosophila* NF-kappaB signaling. — *Mol. Cell* **37**: 172–182.

Park M.-Y., Jang H.D., Lee S.Y., Lee K.-J. & Kim E. 2004: Fas-associated factor-1 inhibits nuclear factor-kappaB (NF-kappaB) activity by interfering with nuclear translocation of the RelA (p65) subunit of NF-kappaB. — *J. Biol. Chem*. **4**: 2544–2549.

Price M.N., Dehal P.S. & Arkin A.P. 2009: FastTree: computing large minimum evolution trees with profiles instead of a distance matrix. — *Mol. Biol. Evol.* **26**: 1641–1650.

Rus F., Flatt T., Tong M., Aggarwal K., Okuda K., Kleino A., Yates E., Tatar M. et al. 2013: Ecdysone triggered PGRP-LC expression controls *Drosophila* innate immunity. — *EMBO J.* **32**: 1626–1638.

Rutschmann S., Jung A.C., Zhou R., Silverman N., Hoffmann J.A. & Ferrandon D. 2000: Role of *Drosophila* IKK gamma in a Toll-independent antibacterial immune response. — *Nat. Immunol.* **1**: 342–347.

Silverman N., Zhou R., Stoven S., Pandey N., Hultmark D. & Maniatis T. 2000: A *Drosophila* I kappa B kinase complex required for Relish cleavage and antibacterial immunity. — *Gen. Dev.* **14**: 2461–2471.

Silverman N., Zhou R., Erlich R.L., Hunter M., Bernstein E., Schneider D. & Maniatis T. 2003: Immune activation of NF-kappa B and JNK requires *Drosophila* TAK1. — *J. Biol. Chem.* **278**: 48928–48934.

Sievers F. & Higgins D.G. 2021: The Clustal Omega Multiple Alignment Package. — *Methods Mol. Biol.* **2231**: 3–16.

Song E.J., Yim S.H., Kim E., Kim N.S. & Lee K.J. 2005: Human Fas-associated factor 1, interacting with ubiquitinated proteins and valosin-containing protein, is involved in the ubiquitin-proteasome pathway. — *Mol. Cell Biol.* **25**: 2511–2524.

Stöven S., Ando I., Kadalayil L., Engstrom Y. & Hultmark D. 2000: Activation of the *Drosophila* NF-kappa B factor Relish by rapid endoproteolytic cleavage. — *EMBO Rep.* **1**: 347–352.

Stöven S., Silverman N., Junell A., Hedengren-Olcott M., Erturk D., Engstrom Y., Maniatis T. & Hultmark D. 2003: Caspase-mediated processing of the *Drosophila* NF-kappa B factor Relish. — *Proc. Natl. Acad. Sci. U.S.A.* **100**: 5991–5996.

Sun H.Y., Bristow B.N., Qu G.W. & Wasserman S.A. 2002: A heterotrimeric death domain complex in Toll signaling. — *Proc. Natl. Acad. Sci. U.S.A.* **99**: 12871–12876.

Tomoyasu Y., Miller S.C., Tomita S., Schoppmeier M., Grossmann D. & Bucher G. 2008: Exploring systemic RNA interference in insects: a genome-wide survey for RNAi genes in *Tribolium*. — *Genome Biol.* **9**: R10, 22 pp.

Tribolium Genome Sequencing Consortium 2008: The genome of the model beetle and pest *Tribolium castaneum*. — *Nature* **452**: 949–955.

Valanne S., Wang J.H. & Rämet M. 2011: The *Drosophila* Toll signaling pathway. — *J. Immunol.* **186**: 649–656.

Verma P. & Tapadia M.G. 2012: Immune response and anti-microbial peptides expression in malpighian tubules of *Drosophila melanogaster* is under developmental regulation. — *PLoS ONE* **7**(7): e40714, 12 pp.

Weber A.N.R., Tauszig-Delamasure S., Hoffmann J.A., Lelievre E., Gascan H., Ray K.P., Morse M.A., Imler J.L. et al. 2003: Binding of the *Drosophila* cytokine Spatzle to Toll is direct and establishes signaling. — *Nat. Immunol.* **4**: 794–800.

Wu L.P. & Anderson K.V. 1998: Regulated nuclear import of Rel proteins in the *Drosophila* immune response. — *Nature* **392**: 93–97.

Yokoi K., Koyama H., Ito W., Minakuchi C., Tanaka T. & Miura K. 2012a: Involvement of NF-κB transcription factors in antimicrobial peptide gene induction in the red flour beetle, *Tribolium castaneum*. — *Dev. Comp. Immunol.* **38**: 342–351.

Yokoi K., Koyama H., Minakuchi C., Tanaka T. & Miura K. 2012b: Antimicrobial peptide gene induction, involvement of Toll and IMD pathways and defense against bacteria in the red flour beetle, *Tribolium castaneum*. — *Results Immunol.* **2**: 72–82.

Zou Z., Evans J.D., Lu Z., Zhao P., Williams M., Sumathipala N., Hetru C., Hultmark D. et al. 2007: Comparative genomic analysis of the *Tribolium* immune system. — *Genome Biol.* **8**: R177.

Received July 19, 2021; revised and accepted December 17, 2021
Published online January 12, 2022

Supplementary figures, supplementary tables and supplementary data

All supplementary figures, supplementary table and supplementary data were uploaded to figshare. DOI: 10.6084/m9.figshare.c.5429688

Supplementary Fig. 1

Approximately-maximum-likelihood phylogenetic trees of (A) Caspar, (B) DREDD and (C) FADD. Numbers near branch points and along the branches are bootstrap values and lengths of branches, respectively. DOI: 10.6084/m9.figshare.14618898

(A) Phylogenetic tree results using the Caspar genes of *T. castaneum* (Tc-caspar), *A. aegypti* (Ae-caspar, GenBank ID: XP_021697938.1), *A. gambiae* (Ag-caspar, GenBank ID: XP_316513), *D. melanogaster* (Dm-caspar, GenBank ID: NP_611080.1), *B. mori* (isoform X1) (Bm-Caspar, GenBank ID: XP_037873675.1), *A. mellifera* (isoform X1) (Am-Caspar, GenBank ID: XP_392750.1), *N. lugens* (Nl-Caspar, GenBank ID: XP_022206141), mouse orthologue FAF1 (Mouse FAF1, GenBank ID: NP_032009.2) and the human orthologue, FAF1 (Human-FAF1, GenBank ID: CAB67705.1). The fasta file of the predicted amino acid sequences is in Supplementary Data 1 (Caspar-AA-seqs.fa),

(B) Phylogenetic tree results using the DREDD genes of *T. castaneum* (Tc-Dredd), *A. aegypti* (Ae-DREDD, GenBank ID: ABI74776.1), *A. gambiae* (Ag-Dredd, GenBank ID: XP_552560.2), *D. melanogaster* (Dm-DREDD (isoform gamma), GenBank ID: AAC33118.1), *B. mori* (Bm-DREDD, GenBank ID: NP_001108337), *A. mellifera* (Am-DREDD, GenBank ID: XP_006570976), *N. lugens* (Nl-DREDD, GenBank ID: XP_039280806), mouse orthologue Caspase-8 (Mouse-Caspase-8, GenBank ID: NP_032009.2) and the human orthologue, Caspase-8 (Hm-Casp8, GenBank ID: AAD24962.1). The fasta file of the predicted amino acid sequences is in Supplementary Data 1 (DREDD-AA-seqs.fa),

(C) Phylogenetic tree results using the FADD genes of *T. castaneum* (Tc-FADD), *A. aegypti* (Ae-FADD, GenBank ID: EAT46931.1), *A. gambiae* (Ag-FADD, GenBank ID: XP_308597.4), *D. melanogaster* (Dm-FADD, GenBank ID: AAF55950.1), *B. mori* (Bm-FADD, GenBank ID: NP_001189465), *A. mellifera* (Am-FADD, GenBank ID: XP_006572135), mouse FADD (Mouse-FADD, GenBank ID: NP_034305) and human FADD (Hm-FADD, GenBank ID: CAG33019.1).The *N. lugens* orthologue was not found in the *N. lugens* genome. The fasta file of the predicted amino acid sequences is in Supplementary Data 1 (FADD-AA-seqs.fa).

Supplementary Fig. 2

InterPro scan results of (A) Tc-Caspar, (B) Tc-DREDD and (C) Tc-FADD. The numbers in the upper part of each figure indicate the sequence numbers of amino acid residues counted from the N terminal end. The gff result file of each amino acid sequence is uploaded in Supplementary Data 3. Detailed results are on the InterPro site (URL: https://www.ebi.ac.uk/interpro/about/interproscan/). DOI: 10.6084/m9.figshare.14625522

Supplementary Table 1

Primer sequence list in the present study. DOI: 10.6084/m9.figshare.14625510

Supplementary Data 1

Fasta files of predicted amino acid sequences of Caspar, DREDD and FADD used for phylogenetic trees. DOI: 10.6084/m9.figshare.16918201

Supplementary Data 2

Aln files (Clustal omega output files) and newick files (FastTree output files) of Caspar, DREDD and FADD. DOI: 10.6084/m9.figshare.14618706

Supplementary Data 3

Gff files of InterProScan results of Tc-Caspar, Tc-DREDD and Tc-FADD. DOI: 10.6084/m9.figshare.16918210